This article was downloaded by:
On: *30 January 2011*
Access details: *Access Details: Free Access*
Publisher *Taylor & Francis*
Informa Ltd Registered in England and Wales Registered Number: 1072954 Registered office: Mortimer House, 37-41 Mortimer Street, London W1T 3JH, UK

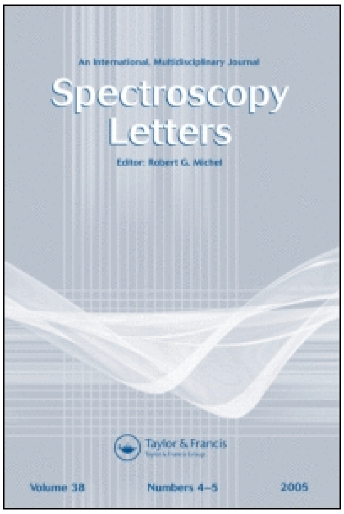

Spectroscopy Letters
Publication details, including instructions for authors and subscription information:
http://www.informaworld.com/smpp/title~content=t713597299

Conformational Dependence of Vibrational Spectra in Some Branched Octanes: 3,3- and 2,2-Dimethylhexanes

S. Mouatarif[a]; C. Van Alsenoy[b]; A. Aboulmouhajir[a]
[a] Equipe de Recherche de Spectroscopie et Chimie Quantique, Faculté des Sciences, Laboratoire de Chimie Physique, Départment de Chimie, Université Chouaib Doukkali, El Jadida, Marocco [b] Structural Chemistry Group, Department of Chemistry, University of Antwerp, Antwerp, Belgium

To cite this Article Mouatarif, S. , Van Alsenoy, C. and Aboulmouhajir, A.(2008) 'Conformational Dependence of Vibrational Spectra in Some Branched Octanes: 3,3- and 2,2-Dimethylhexanes', Spectroscopy Letters, 41: 2, 87 — 99
To link to this Article: DOI: 10.1080/00387010801943954
URL: http://dx.doi.org/10.1080/00387010801943954

PLEASE SCROLL DOWN FOR ARTICLE

Full terms and conditions of use: http://www.informaworld.com/terms-and-conditions-of-access.pdf

This article may be used for research, teaching and private study purposes. Any substantial or systematic reproduction, re-distribution, re-selling, loan or sub-licensing, systematic supply or distribution in any form to anyone is expressly forbidden.

The publisher does not give any warranty express or implied or make any representation that the contents will be complete or accurate or up to date. The accuracy of any instructions, formulae and drug doses should be independently verified with primary sources. The publisher shall not be liable for any loss, actions, claims, proceedings, demand or costs or damages whatsoever or howsoever caused arising directly or indirectly in connection with or arising out of the use of this material.

Spectroscopy Letters, 41:87–99, 2008
Copyright © Taylor & Francis Group, LLC
ISSN: 0038-7010 print/1532-2289 online
DOI: 10.1080/00387010801943954

Conformational Dependence of Vibrational Spectra in Some Branched Octanes: 3,3- and 2,2-Dimethylhexanes*

S. Mouatarif,[1]
C. Van Alsenoy,[2] and
A. Aboulmouhajir[1]
[1]Equipe de Recherche de Spectroscopie et Chimie Quantique, Faculté des Sciences, Laboratoire de Chimie Physique, Départment de Chimie, Université Chouaib Doukkali, El Jadida, Marocco
[2]Structural Chemistry Group, Department of Chemistry, University of Antwerp, Antwerp, Belgium

ABSTRACT As a preliminary study before vibrational analysis, conformational analyses of 3,3- and 2,2-dimethylhexane (3,3-DMH and 2,2-DMH) were done using HF, post-HF, and DFT methods applied to various basis sets. Moreover, computations on a possible rotational barrier from the most stable conformer to the lowest energy secondary conformers were done. The *ab initio* Cartesian force field has been converted to the force field in terms of symmetry coordinates. Normal coordinate calculations were performed using a scaled quantum mechanical (SQM) force field. The scale factors have been optimized in order to reproduce the observed frequencies. Variable temperature study of Raman spectrum of 3,3-DMH in liquid phase was done to confirm the vibrational assignment and to obtain the enthalpy of conformational equilibrium. In addition, the temperature dependence of Raman and IR spectra of 2,2-DMH, made in our previous work, was confronted in this paper with SQM vibrational analysis.

KEYWORDS *ab-initio* analysis, branched octanes, conformational stability, DFT, enthalpy, rotational barriers, vibrational spectra

1. INTRODUCTION

Considering the importance of the branched alkane compounds, it is necessary to identify the right computational method for modeling them, especially their conformational and vibrational properties. The problem of rotational isomerism of the branched alkanes is the first handicap in the analyses of their rich infrared and Raman spectra. Most of these compounds are of particular industrial interest as a molecules for instance, trimethylpentanes, which are used in commercial gasoline to increase the octane number because of their ability to withstand compression and to reduce contribution to pollution, or as a recurring structural subunit of derived polymers like 2,4-dimethylpentane, which is the recurring structural subunit of polypropylene and of many polypropionate-derived natural products. Thereby, the elucidation of the relationship between structure and some physicochemical properties of polymers like rheology,

Received 16 October 2006;
accepted 21 August 2007.

*The authors were invited to contribute this paper to a special issue of the journal entitled "Research on Spectroscopy in Morocco." This special issue was organized by Miguel de la Guardia, Professor of Analytical Chemistry at Valencia University, Spain, and the first group of papers was published in *Spectroscopy Letters*, 40(5), 2007. This article is grouped with other Moroccan papers in volume 41(2), 2008.

Address correspondence to A. Aboulmouhajir, Equipe de Recherche de Spectroscopie et Chimie Quantique, Faculté des Sciences, Laboratoire de Chimie Physique, Départment de Chimie, Université Chouaib Doukkali, B.P. 20, 24000, El Jadida, Marocco.
E-mail: aboulmouhajir@yahoo.fr

Downloaded At: 02:52 30 January 2011

viscosity, or diffusion requires the structural study of monomer.[1–4] Indeed, this procedure allows evaluating the effect of branching, shape, size, and side-chain position on the polymer backbone dimension and especially on the polymer backbone flexibility.[5] In addition, the force field parameterization of branched alkanes could be the basis for developing a spectroscopically reliable molecular mechanics energy function for their derived polymers.[6,7]

In our earlier work, interest was focused on conformational and vibrational analyses of branched octanes. The structures of the most and less-stable conformers, as well as the energy differences between them, were calculated using molecular mechanics and semiempirical methods. For each isomer, a normal mode computation (local symmetry force field) was made to assign a large number of features in its infrared and Raman spectra. Furthermore, by studying the effect of temperature on the vibrational spectra, the enthalpy of equilibrium between conformers was determined for some isomers and compared with theoretical values.[8–12]

Recently, we have tried to obtain an *ab initio* view of the conformational analysis of branched octanes using various levels of theory.[13] The current article presents the conformational dependence of the vibrational spectra of 2,2- and 3,3-DMH. A scaled *ab initio* force field was determined to calculate the normal mode frequencies. The temperature sensitivity of 3,3-DMH Raman spectrum was investigated in order to determine the conformational equilibrium enthalpy, and the temperature sensitivity of 2,2-DMH vibrational spectra[10] is confronted with scaled quantum mechanical (SQM) vibrational analysis.

Downloaded At: 02:52 30 January 2011

2. CONFORMATIONAL ANALYSIS

Because of the importance of the relative stability ordering of conformers, it is necessary to subject their energy difference to various levels of theory. Hartree-Fock theory (HF), Möller-Plesset perturbation theory (MP) and Density functional theory (DFT). In order to investigate the effect of electron correlation, we have performed the MP2, MP3, and MP4(DQ) energy calculations at both HF and MP2 optimized geometry with 6–31G** basis set. Local Density Approximation (LDA) of SUWN functional and various gradient correction schemes (B3P86, B3PW91, B3LYP, BLYP) were also applied. In addition, zero point energy (ZPE) and thermal corrections have been carried out based on HF and DFT (B3LYP) methods. The rotational barriers from the most stable conformer to the lowest energy secondary conformers have also been approached. All calculations were performed using the Gaussian 98 program.[14]

It is difficult to determine *a priori* the most stable conformations of the dimethylhexanes because of the steric hindrance due to the substitution of hydrogen atoms by alkyl groups in the main chain. The carbon positions for each isomer are well-known by evaluating the three central torsional angles $\tau_1 = C_1\text{-}C_2\text{-}C_3\text{-}C_4$, $\tau_2 = C_2\text{-}C_3\text{-}C_4\text{-}C_5$, and $\tau_3 = C_3\text{-}C_4\text{-}C_5\text{-}C_6$. The torsional angle $\tau_1 = C_1\text{-}C_2\text{-}C_3\text{-}C_4$ is taken to be positive if, when looking from C_2 along $C_2\text{-}C_3$ bond, C_4 is in the clockwise sense with respect to C_1. The atom numbering for 3,3-DMH and 2,2-DMH is given in Figure 1.

In order to generate a maximum of combination of terminal group positions, we have assigned 180°, +60°, and −60° to each of torsional angles τ_1, τ_2, and τ_3. Each conformation among 27 possible conformations obtained was then optimized at HF/6-31G without any symmetry constraint and with the use of complete relaxation method.

3,3-DMH, as presented in our earlier work[13] has four stable conformers within 1 Kcal/mol: A($\tau_1 \sim 60$, $\tau_2 \sim 60$, $\tau_3 \sim 180$), B($\tau_1 \sim 60$, $\tau_2 \sim 180$, $\tau_3 \sim 180$), C($\tau_1 \sim 180$, $\tau_2 \sim 60$, $\tau_3 \sim 180$), D($\tau_1 \sim 180$, $\tau_2 \sim 180$, $\tau_3 \sim 180$), and two other less stable conformers, E($\tau_1 \sim 60$, $\tau_2 \sim -90$, $\tau_3 \sim 180$), F($\tau_1 \sim 90$, $\tau_2 \sim -60$, $\tau_3 \sim 180$), with relative energy values superior than 2.5 Kcal/mol because of the syn-pentane interactions.[15]

The calculated HF energy for 2,2-DMH leads only two conformers A($\tau_1 \sim 180$, $\tau_2 \sim 180$, $\tau_3 \sim 180$) and B($\tau_1 \sim 180$, $\tau_2 \sim 180$, $\tau_3 \sim 60$) with a difference

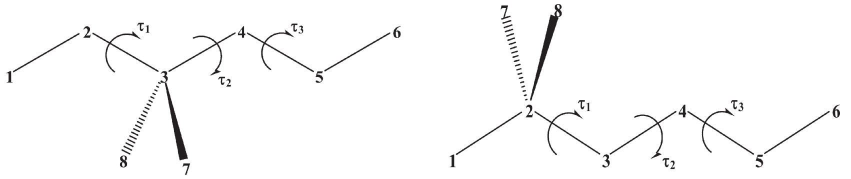

FIGURE 1 Atom Numbering for the Carbon Atoms and Definition of the Central Torsional Angles for 3,3- and 2,2-DMH.

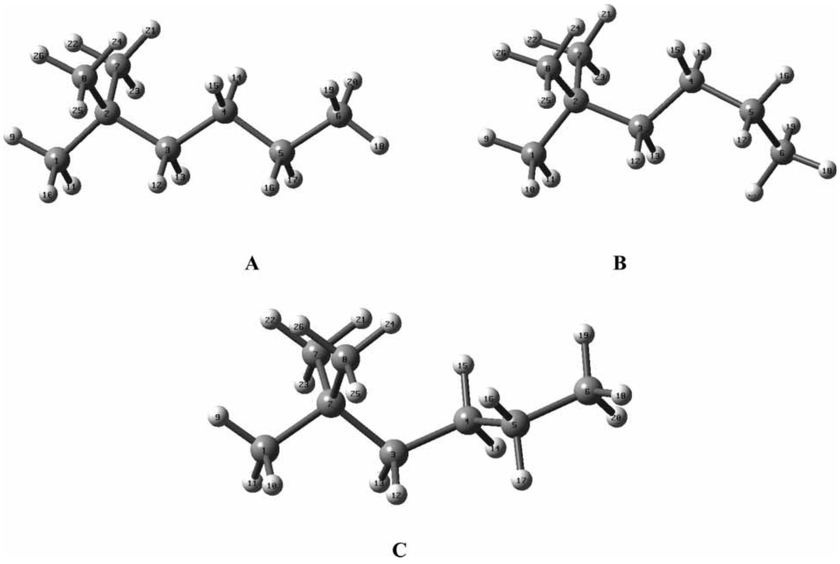

FIGURE 2 MP2/6-31G* Optimized Geometry of Stable Conformers of 2,2-dimethylhexane: A (~180, ~180, ~180), B (~180, ~180, ~60), C (~80, ~100, ~180).

Downloaded At: 02:52 30 January 2011

energy of about 1.1 Kcal/mol and the conformer C ($\tau_1 \sim 80$, $\tau_2 \sim 100$, $\tau_3 \sim 180$) whose HF relative energy value (2.86 Kcal/mol) is so far from A and B that it was ignored (Fig. 2).

The evaluation of ZPE and thermal contributions investigated at both HF/6-31G* and B3LYP/6-31G* leads to believe that they do not have a significant effect on the computed conformational stability ordering. Therefore, all calculations using higher-level methods did not integrate the thermal energy correction.[13,16]

The HF, post-HF, or DFT energy computations of 3,3-DMH conformers show that the conformational stability is insensitive to the extension of basis set from 6-31G to 6-31G** and to the optimization method. However, it is changed in DFT methods compared with HF and post-HF methods. Indeed, in DFT methods, D becomes slightly more stable than B and C conformers. A relative energy increase from HF to MPn was also noticed. On the other hand, except for LDA, which has higher energy values, almost all the relative energy values of the gradient corrected density functionals are relatively comparable with HF energy value.[13] According to these results, we have noticed that some *n*-alkane conformational results are not extrapolated to branched alkanes. Indeed, BLYP applied to 6-31G* does not match with MP4, and the HF relative energy difference does not increase from 6-31G to 6-31G*, theses supported by Tsuzuki et al.[17] and Mirkin and Krimm,[18] respectively.

Contrary to 3,3-DMH, the 2,2-DMH relative energy decreases substantially from HF to MPn methods. Concerning DFT methods, except LDA, which energy values are very weak, the other methods provide relative energy values between those of HF and MPn (Table 1). On the other hand, the insensitivity of the conformational energy difference to the basis sets is also confirmed for this molecule as it does not change significantly even with the extended basis set 6-311++G** especially for the DFT energy calculations (Table 2).

TABLE 1 Electronic Energy (Hartree) of the Most Stable Conformer and a Relative Energy (Kcal/mol) of the Lowest Energy Secondary Conformer of 2,2-DMH Obtained at Various Levels of Theory with 6-31G** Basis Set

Methods	A	B
HF//HF	−313.461401	1.11
HF//MP2	−313.460794	1.21
MP2//HF	−314.640570	0.71
MP3//HF	−314.730689	0.77
MP4(DQ)//HF	−314.735757	0.76
MP2//MP2	−314.641145	0.63
MP3//MP2	−314.730968	0.73
MP4(DQ)//MP2	−314.736114	0.73
B3LYP//HF	−315.734893	0.96
B3P86//B3P86	−316.944778	0.88
B3PW91//B3PW91	−315.623658	0.96
B3LYP//B3LYP	−315.500584	0.99
BLYP//BLYP	−315.736064	0.96
SVWN//SVWN	−313.976044	0.42

TABLE 2 **Conformational Relative Energy (Kcal/mol) of 2,2-DMH at Some Levels of Theory with Different Basis Sets**

Method	6-31G	6-31G**	6-311++G**
HF//HF[a]	1.06	1.11	1.12
MP2//HF	0.81	0.70	0.57
B3LYP//HF	1.00	0.96	0.96
B3P86//B3P86	0.88	0.88	0.85
B3PW91//B3PW91	0.97	0.96	0.94
B3LYP//B3LYP	0.94	1.00	0.97
BLYP//BLYP	0.98	0.97	1.01
SVWN//SVWN	0.42	0.42	0.35

[a] All the optimized geometries are obtained with 6-31G.

The dependence of the structural parameters on the methodology was also investigated. The inclusion of electron correlation, by MP2/6-31G*, decreases CC bond lengths, especially C_2C_3, C_3C_4, C_3C_7, and C_3C_8 for 3,3-DMH and C_1C_2, C_2C_3, C_2C_7, and C_2C_8 for 2,2-DMH of about 0.006 Å, increases CH bond lengths of 0.01 Å, and affect, essentially the central torsional angles, of about ±2°. The MP2/6-31G* optimized CC bonds, CCC valence angles, and the three central torsional angles τ_1, τ_2, and τ_3 have been collected in Table 3. On the other hand, B3LYP/6-31G* increases both CC and CH bond of about 0.004 Å and 0.011 Å, respectively.

TABLE 3 **MP2/6-31G* Optimized Structural Parameters CC, CCC, τ_1,τ_2 and τ_3 of Stable Conformers of 3,3- and 2,2-DMH**

3,3-DMH		2,2-DMH	
Coordinate[a]	Value[b]	Coordinate[a]	Value[b]
R(1,2)	1.528	R(1,2)	1.532
R(2,3)	1.540	R(2,3)	1.539
R(3,4)	1.540	R(2,7)	1.531
R(3,7)	1.532	R(2,8)	1.531
R(3,8)	1.532	R(3,4)	1.528
R(4,5)	1.528	R(4,5)	1.528
R(5,6)	1.528	R(5,6)	1.526
A(1,2,3)	116.2	A(1,2,3)	108.0
A(2,3,4)	111.9	A(1,2,7)	108.8
A(2,3,7)	108.1	A(1,2,8)	108.8
A(2,3,8)	110.2	A(3,2,7)	110.8
A(4,3,7)	110.3	A(3,2,8)	110.8
A(4,3,8)	108.1	A(7,2,8)	109.5
A(7,3,8)	108.1	A(2,3,4)	117.1
A(3,4,5)	116.9	A(3,4,5)	112.2
A(4,5,6)	111.7	A(4,5,6)	112.7
D(1,2,3,4)	55.6	D(1,2,3,4)	180.0
D(2,3,4,5)	55.8	D(2,3,4,5)	−180.0
D(3,4,5,6)	178.3	D(3,4,5,6)	180.0

[a] See Fig. 1 for atom numbering.
[b] Bond lengths in angstrom, bond angles in degrees.

TABLE 4 **Values (Kcal/mol) of Possible Rotational Barriers from the Most Stable Conformer to the Lowest Energy Secondary Conformers and Their Correspondent Inversion (in Parentheses) Barriers**

	3,3-DMH		2,2-DMH
	A → B	A → C	A → B
HF/6-31G*	5.14 (4.76)	5.24 (4.84)	3.56 (2.45)
MP2/6-31G*	5.49 (4.90)	5.69 (5.05)	3.46 (2.70)

The A → B rotational barrier with respect to τ_2, the A → C rotational barrier with respect to τ_1 for 3,3-DMH, and the A → B rotational barrier with respect to τ_3 for 2,2-DMH are calculated at HF/6-31G* and MP2/6-31G*. The calculated barrier heights, with their correspondent inversion barrier values, are collected in Table 4. For these calculations, the variation of torsional angle was made in steps of 5°, that is, the concerned torsional angle τ_1, τ_2, or τ_3 was kept at a constant value and all the other internal coordinates were optimized (Fig. 3 and Fig. 4). Unfortunately, there are no experimental values for these barriers. However, the barrier height of 2,2-DMH could be compared with the butane one, which is calculated as 3.49[19] and 3.31 Kcal/mol[20,21] and determined experimentally as 3.62 Kcal/mol.[22]

3. ENTHALPY OF CONFORMATIONAL EQUILIBRIUM

The determination of the difference in enthalpy between two conformers A and B in equilibrium is made on the basis of Van't Hoff's law:

$$\mathbf{Ln}\frac{I^*_{\mathbf{A}}}{I^*_{\mathbf{B}}}\frac{\Delta \boldsymbol{H}}{\boldsymbol{R}}\cdot\frac{1}{\boldsymbol{T}}+\text{constant}$$

Where the corrected integrated intensities are given by $\boldsymbol{I}^*_{\mathrm{A/B}} = \boldsymbol{I}_{\mathrm{A/B}}\ (1 - e^{-h\nu/kT})$, these quantities are proportional to the total number of molecules in conformers A and B, respectively.[23,24] R is the gas constant and ΔH is the difference in enthalpy between conformers A and B. The integrated intensities were evaluated with the aid of a standard curve-fitting program.

The vibrational spectra temperature sensitivity of 2,2-DMH was studied before, from 800 cm^{-1} down in Raman spectrum and from 600 cm^{-1} to 200 cm^{-1} in infrared spectrum.[10] In this communication, the

Downloaded At: 02:52 30 January 2011

Downloaded At: 02:52 30 January 2011

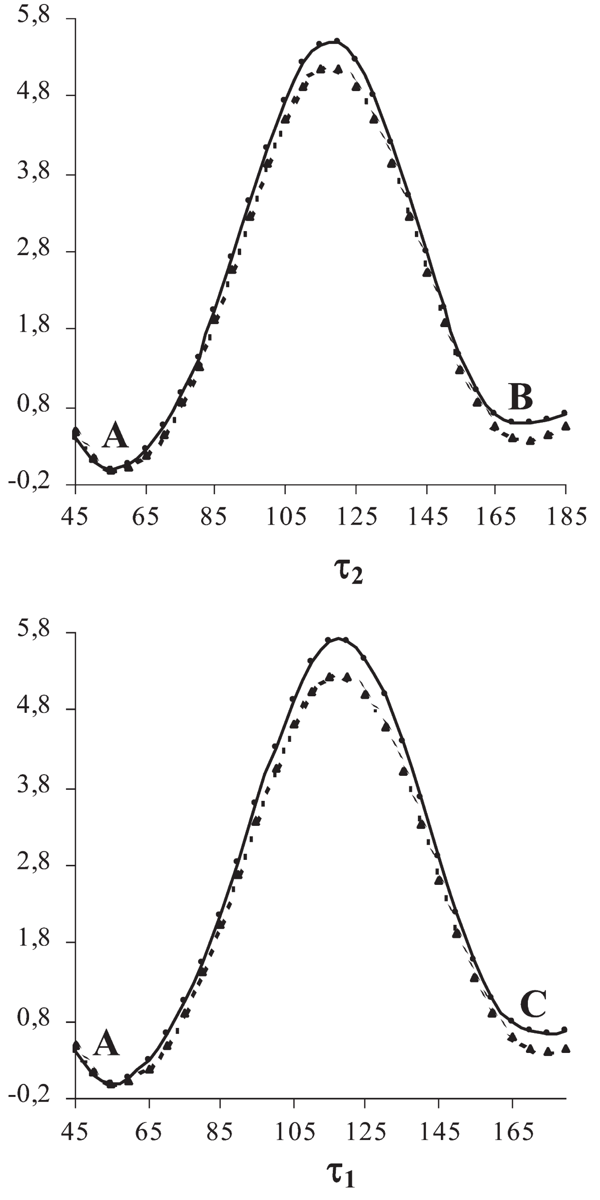

FIGURE 3 HF/6-31G* (Dashed Line) and MP2/6-31G* (Solid Line) Rotational Barriers for 3,3-dimethylhexane. A (~60, ~60, ~180), B (~60, ~180, ~180), C (~180, ~60, ~180).

temperature sensitivity from 800 cm^{-1} down in Raman spectrum of 3,3-DMH is studied. It exhibits only one temperature-sensitive pair of bands at 328 and 343 cm^{-1} (Fig. 5), whereas the Raman and IR spectra of 2,2-DMH present a multitude of sensitive pairs of bands (Fig. 6 and Fig. 7). The band that increases in intensity with decreasing temperature sample is assigned to the most stable conformer. Table 5 reports these pairs of bands and the resulting values of the equilibrium conformational enthalpy in liquid phase. The different measurements of the enthalpy difference between conformers of 2,2-DMH lead to an average value of $\Delta H = 0.74 \pm 0.26$ Kcal/mol.

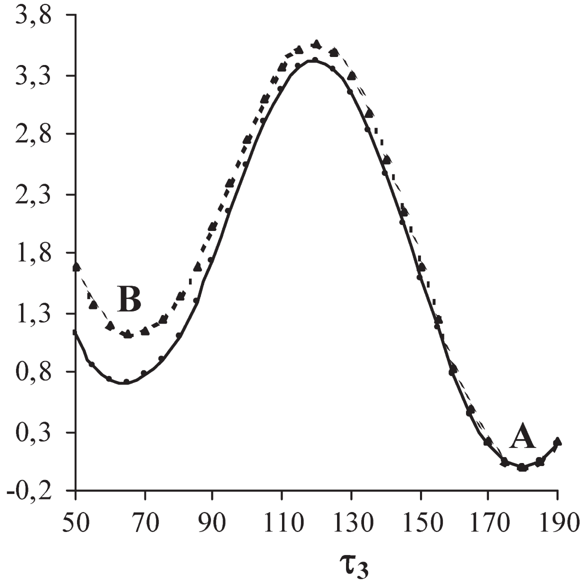

FIGURE 4 HF/6-31G* (Dashed Line) and MP2/6-31G* (Solid Line) Rotational Barrier for 2,2-dimethylhexane. A (~180, ~180, ~180), B (~180, ~180, ~60).

The 3,3-DMH compound investigated in this work (purity > 99%) was purchased from Aldrich and used as received. The Raman spectrum was recorded with a Dilor RT-30, triple-monochromator instrument with the use of a krypton-ion laser ($\lambda = 647.1$ nm) at a power of 300 mw. The resolution was 1 cm^{-1} or better, and five accumulations were made. Under these conditions, the band intensities were considered to be sufficiently reliable for quantitative measurements. The Raman spectrometer was equipped with a low-temperature cryostat controlled to within 2°C. The sample was

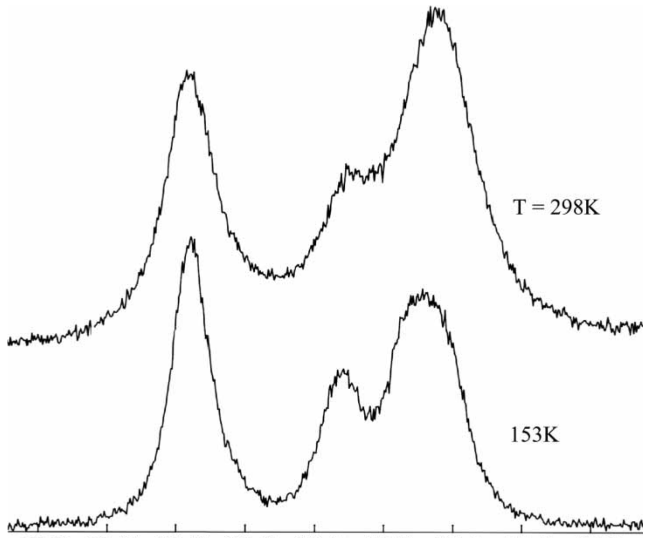

FIGURE 5 Temperature Sensitivity of Raman Bands of 3,3-DMH in Liquid Phase.

Downloaded At: 02:52 30 January 2011

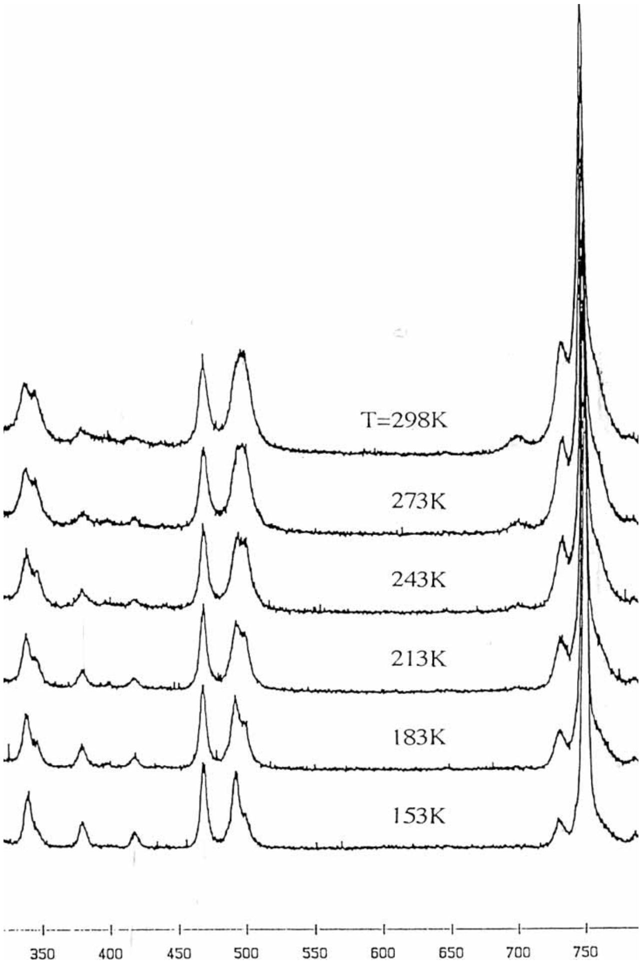

FIGURE 6 **Temperature Sensitivity of Raman Bands of 2,2-DMH in Liquid Phase.**

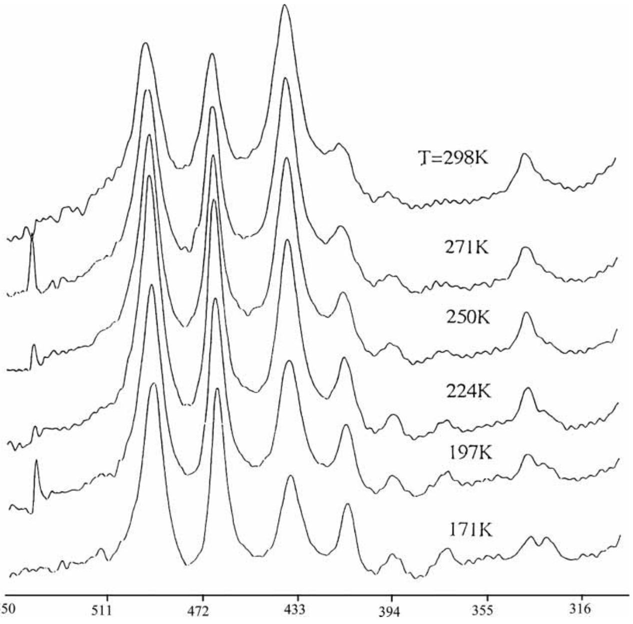

FIGURE 7 **Temperature Sensitivity of Infrared Bands of 2,2-DMH in Liquid Phase.**

TABLE 5 **Vibrational Bands Pairs Sensible to the Temperature and Conformational Enthalpy**

	Pairs of bands		
Molecule	Raman	IR	ΔH (Kcal/mol)
2,2-DMH[b]	338[a]–345		0.78 ± 0.10
	492–499		0.86 ± 0.11
	745–760		0.65 ± 0.08
		418–438	0.73 ± 0.16
		438–468	0.67 ± 0.85
3,3-DMH	343–328		0.280 ± 0.006

[a] The underlined bands correspond with the most stable conformer.
[b] From Ref. [10].

contained in a Pyrex capillary of 2.5 mm diameter. Careful attention was paid to ensure equilibrium at each temperature; reproducible results were obtained in each case after a number of runs.

4. VIBRATIONAL NORMAL MODE CALCULATIONS

A vibrational spectrum depends on a structure. It could be used consequently to confirm a proposed conformation. Because the relationship between them is not direct, empirical formalisms were developed. The Wilson GF method, which is the most used in normal coordinate analysis, has a disadvantage to require a multitude of force constants to describe relatively well the potential energy surface, especially in terms of symmetry coordinates. On the other hand, the *ab initio* calculated frequencies are relatively larger than the corresponding experimental values. This is partly due to neglect of anharmonicity and partly to the approximate nature of quantum mechanical methods (degree of neglect of electron correlation and basis set truncation).

The scaling of the *ab initio* force field and the optimization of its scale factors are performed in order to provide a good agreement between the calculated and observed frequencies. Because it remains sufficiently impregnated by its *ab initio* character, the scaled force field seems to be complete and useful as a basis for the development of spectroscopically accurate molecular mechanics energy function. The studied molecules differ only by a relative position of alkyl groups along the carbon skeleton. Then, the scale factors force constants were determined in terms of symmetry coordinates. Indeed, the vibrational results obtained with these scale factors were found slightly better than those obtained with scale factors defined in terms of internal coordinates for *n*-pentane and *n*-hexane.[18] Moreover, the local symmetry scale factors could be transferred unchanged between the *ab initio* force field conformers. The complete force field in Cartesian coordinates of our branched octanes was determined by *ab initio* molecular orbital calculations using the Gaussian 98 program package[14] at HF/6-31G after optimizing the equilibrium geometries at the same level of theory. Indeed, according to Mirkin and Krimm vibrational analyses on a series of *n*-alkanes and some congested branched alkanes,[18,25] it showed that HF/6-31G gives more accurate results (eigenvectors and interaction force constants) than HF/6-31G* and equivalent to MP2/6-31G*. Recently, B3LYP with 6-31G, 6-31G*, and 6-31G** was tested. We have noticed that B3LYP/6-31G[26] gave a least RMS deviation for non–CH stretching frequencies of 3,3-DMH compared with B3LYP using 6-31G* or 6-31G** and also to HF/6-31G. Then, we have tried to extend this procedure to other molecules.[27] The Cartesian force field has been converted to the force field in local symmetry coordinates. The scale factors of *ab initio* calculations were optimized and are listed in Table 6. We notice that the 2,2- and 3,3-DMH scale factors values are almost the same as those obtained by Mirkin and Krimm[18,25] except for CCC coordinate and especially for CC torsional coordinate. For the latter coordinate, Mirkin retains the same scale factor value for *n*-alkanes and some branched alkanes even if they are congested like neopentane and 2,2-dimethylbutane.

Downloaded At: 02:52 30 January 2011

TABLE 6 **Local Symmetry Coordinate Scale Factors to HF/6-31G Force Constants for 2,2- and 3,3-DMH**

Symmetry coordinate	Scale factor
CCs	0.869
CH3s	0.829
CH2s	0.813
CH3sb	0.760
CH3ab	0.779
CH3r	0.772
CH2b	0.778
CH2ro	0.795
CH2wa	0.775
CH2tw	0.783
CCCb	0.817
CCt	1.078

Supported by the evaluation of the potential energy distribution (PED) contributions, the vibrational normal modes calculated with the scaled quantum mechanical force field for the most stable conformer of 2,2- and 3,3-DMH were identified with the experimentally observed modes. On the other hand, in order to confirm the assignment of the temperature-sensitive bands, the normal mode analysis with the same scaled force field, assumed unchanged, was made for the lowest energy secondary conformers. The observed frequencies as well as the calculated frequencies for two stable conformers of 2,2-DMH and four stable conformers of 3,3-DMH are given in Tables 7 and 8, respectively. The PED (contributions ≥ 10) for the most stable conformer is given, except when its band does not exist; in which case the PED listed is for the lowest energy conformer. Generally, the computed scaled frequencies are in good agreement with the experimental data leading RMS deviation that does not exceed 4.6 cm^{-1} for frequencies below 1500 cm^{-1}. While the empirical vibrational analysis separates the stretching modes of methyl and methylene in terms of frequencies and PED, the scaled *ab initio* vibrational analysis gives the asymmetric stretching mode of CH_2 (CH_2as) and symmetric stretching mode of CH_3 (CH_3ss) in the same region 2920–2870 cm^{-1}. On the contrary, the asymmetric stretching mode of CH_3 (CH_3as) and symmetric stretching mode of CH_2 (CH_2ss) are purely expressed and calculated in the region 2980–2950 cm^{-1} and 2870–2840 cm^{-1}, respectively. On the other hand, the scaled *ab initio* force field leads, like the empirical force field, the asymmetric bending of CH_3 (CH_3ab) and symmetric bending of CH_2 (scissoring), which often contribute to the same mode in the region 1480–1440 cm^{-1}. A quasi-pure symmetric bending of CH_3 is found in the region 1390–1360 cm^{-1} and the wagging (wa) and twisting (tw) modes of CH_2 are present dominantly in the region 1360–1250 cm^{-1}. From 1250 to 800 cm^{-1}, CC stretching is combined, in most of the cases, with methyl rocking while it expresses solely from 800 to 600 cm^{-1}. The frequencies modes of CCC bending and torsion are obviously evaluated below 600 cm^{-1}. The central CCC deformation and CC torsion frequencies were calculated lower than the terminal ones. The tertiobutyl group $C(CH_3)_3$ and internal isopropyl group $C(CH_3)_2$ have an intense symmetric stretching polarized band in Raman. It is observed at 745,

TABLE 7 **Observed and Calculated Frequencies (CM^{-1}) of 2,2-DMH**

ν(Obs)		ν(Calc)		
Raman	IR	A	B	Potential energy distribution[a]
2961	2954	2967	2964	C8H3as2(37)C7H3as2(37)C8H3as1(11) C7H3as1(11)
2961	2954	2961	2960	C7H3as2(30)C8H3as2(30)C7H3as1(17) C8H3as1(17)
2961	2954	2956	2958	C1H3as1(53)C7H3as1(19)C8H3as1(19)
2961	2954	2954	2952	C6H3as1(98)
2961	2954	2952	2948	C6H3as2(43)C1H3as2(40)
2961	2954	2951	2947	C6H3as2(48)C1H3as2(40)
2961	2954	2946	2942	C1H3as1(46)C7H3as1(19)C8H3as1(19)
2961	2954	2945	2942	C8H3as1(30)C7H3as1(30)C1H3as2(16) C8H3as2(12)C7H3as2(12)
2939	2930	2916	2917	C4H2as(66)C5H2as(14)C3H2as(10)
2886	2890	2898	2897	C7H3ss(38)C8H3ss(38)C1H3ss(18)
2886	2890	2891	2893	C6H3ss(97)
2886	2890	2889	2890	C8H3ss(46)C7H3ss(46)
2886	2890	2886	2886	C1H3ss(80)
2886	2890	2883	2884	C5H2as(73)C4H2as(13)
2878	2873	2875	2882	C3H2as(81)C4H2as(16)
2878	2873	2873	2872	C4H2ss(90)
2865	2863	2862	2862	C5H2ss(87)
2848	2843	2847	2852	C3H2ss(92)
1468	1474	1478	1478	C1H3ab1(22)C7H3ab1(21)C8H3ab1(21)
1468	1470	1473	1471	C5H2b(31)C4H2b(22)C6H3ab1(19)
1468	1470	1470	1470	C1H3ab2(44)C7H3ab1(23)C8H3ab1(23)
1468	1470	1470	1469	C8H3ab2(20)C7H3aba2(20)C8H3ab1(15) C7H3ab1(15)
1468	1460	1462	1465	C6H3ab2(93)
1468	1460	1461	1461	C6H3ab1(56)C4H2b(24)C3H2b(10)
1452	1454[b]	1457	1457	C1H3ab1(37)C4H2b(21)C5H2b(17)
1452	1454[b]	1455	1454	C1H3ab2(29)C7H3ab1(16)C8H3ab1(16) C7H3aba2(16)C8H3ab2(16)
1452	1454[b]	1453	1453	C5H2b(44)C1H3ab1(14)C3H2b(11)
1452	1454[b]	1448	1448	C7H3aba2(31)C8H3ab2(31)C1H3ab2(18)
1452	1454[b]	1447	1446	C3H2b(53)C1H3ab1(15)C4H2b(12)
1391[b]	1392	1390	1390	C8H3sb(30)C7H3sb(30)C1H3sb(28)
1378[b]	1380	1377	1378	C6H3sb(86)
1367	1364	1366	1367	C7H3sb(45)C8H3sb(45)
1367	1364	1365	1366	C1H3sb(46)C8H3sb(13)C7H3sb(13)
1367	1364	1360	1361	C4H2wa(25)C3H2wa(21)C1H3sb(16)
1344	1339	1343	1342	C5H2wa(46)C3H2wa(30)
1318	1315	1317	1315	C3H2tw(55)C4H2tw(16)
1305	1297	1296	1311	C5H2tw(51)C4H2tw(34)
		1283	1275	C4H2wa(33)C5H2wa(16)C3H2wa(11)
1271	1269	1269	1265	C2C3s(24)SD(17)C1H3r1(10)
1252	1250	1252	1256	C5H2tw(21)C4H2tw(18)C3H2ro(11)
		1227	1218	C5H2ro(21)C6H3r2(20)C4H2ro(14)C3H2tw(11)
1206	1205	1210		C1C2s(20)C3H2wa(14)
1190			1197	C3H2tw(14)C4H2ro(12)C4H2tw(10)
1106	1105	1101	1112	C6H3r1(24)C4C5s(15)C3C4s(11)
1097	1092	1096	1099	C3H2tw(20)C1H3r2(18)
1067	1065	1067	1073	C4C5s(37)C3C4s(35)C5C6s(14)
1033	1029	1031	1029	C5C6s(46)C1H3r1(15)C3C4s(12)
1015	1011	1013	1015	C3C4s(18)C1H3r1(18)C8H3r1(15)C7H3ar1(15)
1015	1011	1011		C7H3ar2(21)C8H3r2(21)C3H2tw(11)C4H2tw(10)
991			989	C3C4s(34)C2C3s(13)C5C6s(10)

(*continued*)

Downloaded At: 02:52 30 January 2011

TABLE 7 Continued

ν(Obs)		ν(Calc)		
Raman	IR	A	B	Potential energy distribution[a]
		941	947	C1H3r2(34)C7H3ar1(23)C8H3r1(23)
933	932	929	933	C1H3r2(14)C7H3ar1(14)C8H3r1(14) C2C8s(13) C2C7s(13)
933	932	925	927	C1H3r1(28)C1C2s(14)
913	908	914	915	C6H3r2(21)C5H2tw(15)C3H2ro(15)C4H2ro(13) C2C7s(11)C2C8s(11)
913	908	902		C2C3s(28)C1C2s(27)
896	894	886	900	C6H3r1(33)C4C5s(27)C5C6s(15)
877	873		865	C5C6s(34)C4C5s(31)
787	789	797	783	C3H2ro(28)C5H2ro(23)C6H3r2(20)
760			755	C4H2ro(19)C2C7s(17)C3H2ro(16)
745		746		C2C8s(28)C2C7s(28)C1C2s(16)C2C3s(15)
737	731	736	723	C4H2ro(36)C5H2ro(33)
499	496		500	SD(36)C2C3C4b(12)
492	493	486		SD(23)C2C3C4b(22)R1(16)
468	468	466		SD(36)C4C5C6b(15)C3C4C5b(13)R1(12)
436	438		443	R1(25)AD1(18)C3C4C5b(15)C4C5C6b(14)
417	418	421	421	AD2(40)R2(37)
400	400		396	C4C5C6b(35)SD(27)
379	380	365		AD1(61)C4C5C6b(17)
345	346		341	AD1(52)R1(20)
338	340	337	336	R2(42)AD2(38)
306	300	303		C2C7t(22)C2C8t(22)SD(11)C3C4C5b(11)
292	292	297	293	C1C2t(45)C2C8t(17)C2C7t(17)
292	292		290	R1(37)C4C5C6b(20)AD1(18)
		284	282	R1(37)C4C5C6b(20)AD1(18)
267	270	269		C2C8t(25)C2C7t(25)C3C4C5b(13)SD(12)
		254	247	C5C6t(50)C1C2t(26)
237	237	249	239	C5C6t(35)C1C2t(22)C2C7t(19)C2C8t(19)
			171	C2C3C4b(32)C3C4C5b(23)C5C6t(15)R1(13)
138		143		C4C5t(40)C2C3t(30)
		123	126	C2C3C4b(36)C3C4C5b(35)C4C5C6b(17)
96		83	95	C3C4t(59)C4C5t(15)
		51		C2C3t(45)C3C4t(31)C4C5t(11)
			32	C3C4t(45)C2C3t(31)C4C5t(15)

CH_3as_1 (CH_3as_2), in plane (out of plane) degenerate stretching of CH_3; CH_3ss, totally symmetric stretching of CH_3; CH_3sb, totally symmetric bending of CH_3; CH_3ab_1 (CH_3ab_2), in plane (out of plane) degenerate bending of CH_3; CH_3r_1 (CH_3r_2), in plane (out of plane) degenerate rocking of CH_3; CH_2as, asymmetric stretching of CH_2; CH_2ss, symmetric stretching of CH_2; CH_2b, scissoring of CH_2; CH_2tw, twisting of CH_2; CH_2ro, rocking of CH_2; CH_2wa, wagging of CH_2; AD_1 (AD_2), in plane (out of plane) degenerate bending of tertiobutyl; SD, totally symmetric bending of tertiobutyl; CCs, CC stretching; CCCb, CCC bending; CCt, CC torsion.

[a] Potential energy distribution (contribution ≥ 10) for A conformer, except when no A band is given, in which case the PED is for the B conformer.

[b] From Ref. [28].

Downloaded At: 02:52 30 January 2011

717 cm^{-1} and calculated at 746, 713 cm^{-1} for 2,2- and 3,3-DMH, respectively.

The vibrational analysis of 2,2-DMH confirms the band assignment deduced from the temperature sensitivity spectra study. Indeed, the bands that decrease in intensity with decreasing sample temperature (Fig. 6), observed at 760, 499, 436, 400, and 345 cm^{-1}, correspond actually with the conformer B and are calculated at 755, 500, 443, 396, and 341 cm^{-1}, respectively. Moreover, we have noticed for the region above 800 cm^{-1}, which is not explored by the temperature effect, the presence of other B-specific bands observed at 877, 991, 1190 cm^{-1} and calculated at 865, 989, 1197 cm^{-1}, respectively. On the other hand, the normal modes computation does not reproduce the very weak band observed at 703 cm^{-1}. In opposition to B-specific bands, its intensity disappears totally from 213 K. Then, it leads us to believe that it is

Table 8 **Observed and Calculated Frequencies (CM^{-1}) of 3,3-DMH**

ν(Obs)		ν(calc)				
Ram	IR	A	B	C	D	Potential energy distribution^a
2970	2970	2981	2981	2982	2983	C1H3as2(73)C8H3as1(22)
2970	2970	2973	2975	2977	2980	C7H3as1(78)C8H3as1(14)
2970	2970	2971	2971	2969	2970	C8H3as1(45)C1H3as2(20)C7H3as1(16)C1H3as1(12)
2970	2970	2963	2964	2962	2969	C1H3as1(56)C6H3as1(22)C8H3as1(12)
2970	2970	2963	2961	2961	2963	C6H3as1(59)C1H3as1(26)
2970	2970	2962	2960	2960	2961	C7H3as2(37)C8H3as2(36)C6H3as1(16)
2970	2970	2960	2959	2959	2960	C6H3as2(79)
2970	2970	2954	2955	2955	2960	C7H3as2(51)C8H3as2(49)
2910	2902	2912	2917	2917	2916	C1H3ss(88)
2910	2902	2909	2910	2911	2912	C5H2as(61)C7H3ss(17)
2889		2904	2905	2904	2906	C8H3ss(39)C7H3ss(31)C5H2as(13)
2889		2899	2897	2901	2900	C6H3ss(97)
2889		2898	2897	2898	2898	C8H3ss(48)C7H3ss(46)
2889		2889	2890	2897	2889	C2H2as(77)
2879	2871	2876	2885	2880	2881	C4H2as(72)C5H2as(16)
2879	2871	2872	2880	2874	2873	C5H2ss(90)
2855	2853	2856	2857	2859	2858	C2H2ss(85)
2855	2853	2847	2849	2846	2845	C4H2ss(84)
1470	1475	1479	1478	1477	1481	C8H3ab2(25)C7H3ab2(24)C4H2b(17)
1470	1475	1475	1473	1475	1477	C5H2b(22)C2H2b(16)C1H3ab1(13)C4H2b(12)C8H3ab2(10)
1470	1475	1471	1469	1473	1471	C1H3ab2(39)C2H2b(13)C7H3ab1(11)
1468	1464	1468	1469	1470	1469	C2H2b(25)C8H3ab1(15)C5H2b(13)
1468	1464	1466	1468	1467	1467	C1H3ab1(28)C8H3ab1(25)C5H2b(13)
1468	1464	1463	1465	1463	1463	C7H3ab1(35)C1H3ab2(23)
1468	1464	1461	1462	1459	1460	C6H3ab2(86)
1456	1458	1460	1458	1458	1458	C6H3ab1(22)C8H3ab2(18)C5H2b(16)C7H3ab2(13)C2H2b(11)
1456	1458	1459	1454	1454	1453	C6H3ab1(41)C4H2b(19)C1H3ab1(11)
1456	1458	1453	1449	1451	1451	C8H3ab1(23)C7H3ab2(19)C8H3ab2(18)C2H2b(15)
1441	1449	1449	1447	1446	1443	C7H3ab1(27)C4H2b(23)C8H3ab1(18)
1386^b	1385	1385	1385	1386	1387	C8H3sb(36)C7H3sb(31)
1377	1377	1378	1378	1377	1378	C1H3sb(81)
1377	1377	1377	1376	1375	1375	C6H3sb(75)
1363^b	1365	1365	1366	1366	1367	C7H3sb(37)C8H3sb(18)C5H2wa(14)C4H2wa(11)
1355		1362	1359	1361	1360	C8H3sb(25)C4H2wa(21)C5H2wa(13)
1340^b	1340^b	1350	1348	1343	1342	C2H2wa(59)
1340^b	1340^b				1341	C2H2wa(62)
1328	1330		1324	1325		C2H2tw(25)C4H2tw(20)C2H2wa(14)
1317^b	1322	1314				C5H2wa(43)C4H2wa(17)C2H2tw(12)
1307^b	1310	1306	1305	1313	1306	C4H2tw(41)C5H2tw(24)
1300	1300	1292	1302	1298	1292	C2H2tw(34)C4H2wa(14)
1272	1262	1266	1268	1269		C5H2tw(35)
1255	1261				1255	C4H2tw(25)C2H2tw(24)C5H2tw(16)
		1242			1248	C3C4s(14)
1230^b	1227		1234	1226		C3C4s(16)C2H2ro(12)C1H3r2(11)
1230^b	1227		1222	1225	1219	C3C4s(16)C2H2ro(12)C1H3r2(11)
1208	1213	1213				C5H2ro(10)
1200^b	1191	1202	1204	1206	1203	RO(16)C3C8s(12)C3C7s(12)
1096	1101	1104	1109	1108	1107	C4C5s(27)C6H3r1(19)
1080	1091	1098	1096	1098	1105	C4H2tw(9)C8H3r1(9)C2H2ro(9)C1H3r2(8)
1044	1053	1056	1053	1054	1053	C1C2s(37)C1H3r1(16)C4C5s(13)

(*continued*)

Downloaded At: 02:52 30 January 2011

TABLE 8 **Continued**

ν(Obs)		ν(calc)				
Ram	IR	A	B	C	D	Potential energy distribution^a
1036		1037	1046	1041	1047	C5C6s(51)C6H3r1(12)
1015^b	1018	1018	1023	1021	1020	C4H2tw(13)C1H3r2(11)C2H2tw(10)
1015^b	1018			1018		C1C2s(17)C8H3r1(12)C7H3r2(12)
1010	1007	1007	1004		1009	C1H3r1(28)C1C2s(19)C8H3r2(17)
990	983	988	989	983	983	C7H3r2(33)C8H3r2(31)C1H3r1(12)
952	942	948	958	950	953	C3C4s(24)C8H3r1(17)C5C6s(17)
934	927	927	929	928	929	C7H3r1(35)C8H3r1(23)C3C8s(20)C3C7s(11)
911	908	902	906	906	913	C3C8s(12)
874	878	869		870		C6H3r1(18)C4C5s(14)C3C4s(12)
			859		857	C2C3s(23)C3C4s(11)
848	855	849	849	850	840	C6H3r2(22)C4H2ro(21)C3C7s(11)C2C3s(10)C5H2tw(10)
785	782	779	776	778	776	C2H2ro(44)C1H3r2(34)
730	742	740	740	738	736	C5H2ro(49)C4H2ro(20)C6H3r2(12)
725	724^b		722		722	C3C8s(23)C2C3s(17)C3C7s(16)C3C4s(11)
717		713		707		C2C3s(31)C3C7s(12)C3C4s(11)C3C8s(11)
543	545^b			546	544	WA(24)C1C2C3b(17)C3C4C5b(11)
506	510^b		505			C1C2C3b(24)WA(21)RO(11)
492	502^b	497				C2C3C4b(26)SC(12)C3C4C5b(12)
465	475^b	479	468			RO(31)C1C2C3b(20)WA(11)
437	437			437		RO(37)WA(16)
415	420^b				414	RO(71)
415	420^b	415	416	413	412	WA(44)RO(15)C4C5C6b(13)
367	370^b	361	352	356	359	TW(32)SC(28)C1C2C3b(11)
343	340^b	336	335	335		SC(34)C2C3C4b(22)TW(22)
328	325^b				330	TW(72)
328	325^b	328	325	323	323	C4C5C6b(27)C1C2t(11)
		310	292	304	302	C3C7t(43)C3C8t(39)
					297	C4C5C6b(33)SC(20)C1C2C3b(12)
267	270^b	270	278	283		C5C6t(40)C3C8t(23)TW(11)
267	270^b		265		264	C5C6t(50)C1C2t(12)
		259		257		C3C7t(50)C5C6t(14)
		250	248	249	253	C5C6t(27)C1C2C3b(24)C4C5C6b(10)
		240	241			C3C8t(30)C1C2t(30)C1C2C3b(13)
				222	218	C1C2t(37)C3C8t(28)C3C7t(21)
182		178		174		C3C4C5b(48)C4C5C6b(22)TW(11)
			163			C3C4C5b(32)C2C3C4b(24)C4C5C6b(17)
					152	C3C4C5b(36)C2C3C4b(30)C4C5C6b(18)
		143				C2C3t(38)C1C2t(28)C3C4t(18)
				121		C3C4t(29)C2C3t(20)C1C2t(14)
			108		105	C3C4t(37)C4C5t(18)C3C8t(11)
94		94	92			C3C4t(53)C2C3t(17)
				73	79	C2C3t(51)C4C5t(20)C1C2t(11)
		71				C4C5t(54)C2C3t(23)
			56	61		C3C4t(41)C4C5t(22)C2C3t(20)
					37	C3C4t(36)C2C3t(24)C4C5t(15)

TW, twisting of isopropyl; SC, scissoring of isopropyl; WA, wagging of isopropyl; RO, rocking of isopropyl. See Table 7 for the other abbreviations.

[a] Potential energy distribution (contribution ≥10) for stable conformer A, except when no A band is given, in which case the PED is for the lowest energy conformer.

[b] From Ref. [29].

Downloaded At: 02:52 30 January 2011

characteristic of a secondary conformer C whose a relative energy was evaluated as 2.86 Kcal/mol.

The 2,2-DMH has only two conformers that express spectroscopically but a multitude of a conformational specific bands. On the contrary, the 3,3-DMH has several conformers but few bands with conformational specificity. Indeed, the vibrational computed frequencies of this molecule have reproduced the overall observed bands as common bands of A, B, C, and D conformers, except the two bands observed at 343 and 328 cm^{-1}. The calculated frequencies of A, B, and C conformers, positioned at 335 cm^{-1} and related essentially to the isopropyl CCC deformation, could be identified with the experimental band observed at 343 cm^{-1}, whereas the same nature mode of D calculated at 330 cm^{-1} is identified with the experimental band observed at 328 cm^{-1}. Moreover, this later observed band coincides with all A, B, C, and D modes calculated at about 324 cm^{-1} and related essentially to the CCC deformation associated with CH_2. Consequently, the conformational effect of a decrease of the temperature is an increase of a transformation of D conformer to the most stable conformer A (Fig. 5).

Downloaded At: 02:52 30 January 2011

5. CONCLUSIONS

The current study has been an attempt to elucidate the relative stability of two branched octanes, 2,2- and 3,3-DMH, using a variety of quantum mechanical methods. The ordering of secondary conformers is found to be sensitive to the methodology adopted for 3,3-DMH. Moreover, the differences between HF, MPn (n = 2, 3, 4), and DFT conformational relative energy values is found to be specific to each molecule. The excessive LDA relative energy values leads us to believe that this method is inadequate to model the electronic correlation for this class of compounds.

Concerning the vibrational analysis, a scaled HF/6-31G force field with only a set of 12 scale factors was used in terms of symmetry coordinates. A good agreement between calculated and observed frequencies was obtained as RMS deviation does not exceed 4.6 cm^{-1} for frequencies below 1500 cm^{-1}. The transferability of such set of scale factors values was investigated for other series of branched octanes,[27] By studying the effect of temperature on Raman and infrared spectral region low-frequency, the assignment of the stable conformers was made. The conformational equilibrium enthalpy was confirmed between A and B for 2,2-DMH, determined and related to a conformational change between A and D for 3,3-DMH. On the base of our branched octanes results, we project to study the surrounding effect on branched alkanes flexibility and also the derived polymer flexibility.

REFERENCES

1. Doston, N. A.; Galavan, R. L.; Laurence, R.; Tirrell, M. *Polymerization Process Modeling Press*; VCH: New York, 1996.
2. Wescott, J. T.; Hanna, S. The influence of flexible side chains on the dimensions pf flexible polymers. *Computat. Theor. Polymer Sci.* **1999,** *9*, 307.
3. Bhardwaj, I. S. *Polymer Science/Recent Advances*; Editions TECHNIP: Paris, 1994.
4. Lahtela, M.; Linnolahti, M.; Pakkanen, T. A.; Rowley, R. L. Computer simulations of branched alkanes: The effect of side chain and its position on rheological behaviour. *J. Chem. Phys.* **1998,** *108*, 2626.
5. Jabbarzadeh, A.; Atkinson, J. D.; Tanner, R. I. The effect of branching on slip and rheological properties of lubricants in molecular dynamics simulation of Couette shear flow. *Tribiology Int.* **2002,** *35*, 35.
6. Hélio, F. MNDO/AM1/PM3 quantum mechanical semiempirical and molecular mechanics barriers to internal rotation: A comparative study. *J. Mol. Struct. (Theochem)* **1995,** *335*, 129.
7. Palmo, K.; Mirkin, N. G.; Krimm, S. Spectroscopically determined force fields for macromolecules. 2. Saturated Hydrocarbon chains. *J. Phys. Chem. A.* **1998,** *102*, 6448.
8. Aboulmouhajir, A.; Turell, G. Conformational stability of some branched octanes. *J. Mol. Struct.* **1993,** *293*, 31.
9. Aboulmouhajir, A.; Adil, A.; Turell, G. Vibrational and conformational analyses of a series of branched octanes. I. 2,2,3 - trimethyl pentane. *J. Mol. Struct.* **1995,** *349*, 365.
10. Aboulmouhajir, A.; Turell, G. Vibrational and conformational analyses of a series of branched octanes II. 2,2- and 2,5-dimethylhexanes. *Spectrochim. Acta A* **1996,** *52*, 1717.
11. Mouatarif, S.; El Alaoui El Abdellaoui, H.; Aboulmouhajir, A. Theoritical and spectroscopic studies of branched alkanes flexibility. Contribution to the structural study of flexible polymers. *Phys. Chem. News* **2005,** *22*, 95.
12. Aboulmouhajir, A.; Turell, G. Conformational stability and vibrational analysis of a series of branched octanes III: trimethyl pentanes. *Spectrochim. Acta A.* **1999,** *55*, 1453.
13. Mouatarif, S.; Aboulmouhajir, A. An *ab initio* and DFT study of the conformational stability in branched alkanes: illustration for 3,3-dimethylhexane. *J. Mol. Struct. (Theochem)* **2004,** *709*, 157.
14. Frisch, M. J.; Trucks, G. W.; Schlegel, H. B.; et al. *Gaussian*; Gaussian, Inc.: Pittsburgh PA, 2001.
15. Hoffman, R. W.; Menzel, K. Conformational analysis of meso-2,3,4,5-Tetramethylhexane and some of its derivatives. *Eur. J. Org. Chem.* **2001,** *14*, 2749.
16. Koglin, E.; Meier, R. J. An ab-initio study of the relative stability of the ggg and the gtg conformer in hexane. *Chem. Phys. Lett.* **1999,** *312*, 284.
17. Tsuzuki, S.; Uchimaru, T.; Tanabe, K. Conformational analysis of n-alkanes using density functional theory. Comparison with *ab initio* calculations. *Chem. Phys. Lett.* **1995,** *246*, 9.

18. Mirkin, N. G.; Krimm, S. Ab initio studies of the conformational dependence of the spectra of stable conformers of n-pentane and n-hexane. *J. Phys. Chem.* **1993,** *97*, 13887.
19. Murko, M. A.; Castejon, H.; Wiberg, K. B. Carbon-carbon rotational barriers in butane, 1-butene, and 1,3-butadiene. *J. Phys. Chem.* **1996,** *100*, 16162.
20. Smith, G. D.; Jaffe, R. J. Quantum chemistry study of conformational energies and rotational energy barriers in *n*-alkanes. *J. Phys. Chem.* **1996,** *100*, 18718.
21. Allinger, N. L.; Fermann, J. T.; Allen, W. D.; Schaefer III, H. F. The torsional conformations of butane: Definitive energetics from *ab initio* methods. *J. Chem. Phys.* **1997,** *106*, 5143.
22. Herrebout, W. A.; van der Veken, B. J.; Wang, A.; Durig, J. R. Enthalpy Difference between Conformers of *n*-butane and the potential function governing conformational interchange. *J. Phys. Chem.* **1995,** *99*, 578.
23. Colombo, L.; Zerbi, G. Enthalpy difference of rotational isomers in liquid butane and pentane from infrared spectra. *J. Chem. Phys.* **1980,** *73*, 2013.
24. Scherer, J. R.; Snyder, R. G. Raman spectra of liquid *n*-alkanes. II. Longitudinal acoustic modes and the *gauche–trans* energy difference. *J. Chem Phys.* **1980,** *72*, 5798.
25. Mirkin, N. G.; Krimm, S. Ab initio analysis of the vibrational spectra of conformers of some branched alkanes. *J. Mol. Struct.* **2000,** *550*, 145.
26. Liu, F. L.; Xie, Y.; Dai, L. H.; Peng, L. Theoretical study on the molecule $C_{30}H_{20}$: five carbon−carbon single bonds linking a dodecahedrane cage and a pentaprismane cage. *J. Mol. Struct.* **2004,** *710*, 25.
27. Mouatarif, S.; Alsenoy, C. V.; Aboulmouhajir, A. (in preparation).
28. Crowder, G. A.; Jaiswal, R. M. P. Vibrational analysis of some dimethylhexanes. *J. Mol. Struct.* **1983,** *102*, 145.
29. Crowder, G. A. Conformational analysis of 3,3-dimethylhexane. *Spectrosc. Lett.* **1986,** *19*, 783.

Downloaded At: 02:52 30 January 2011